Structural and functional analysis of *APOA5* mutations identified in patients with severe hypertriglyceridemia[S]

Elena Mendoza-Barberá,[1,*] Josep Julve,[1,*,†] Stefan K. Nilsson,[1,§] Aivar Lookene,[**] Jesús M. Martín-Campos,[*] Rosa Roig,[*] Alfonso M. Lechuga-Sancho,[††] John H. Sloan,[§§] Pablo Fuentes-Prior,[2,*] and Francisco Blanco-Vaca[2,*,†,*]**

Institute for Biomedical Research (IIB) Sant Pau,* 08025 Barcelona, Spain; CIBER de Diabetes y Enfermedades Metabólicas Asociadas,† 08017 Barcelona, Spain; Department of Medical Biosciences/Physiological Chemistry,§ Umeå University, SE90187, Sweden; Department of Chemistry,** Tallinn Technical University, Tallinn 12618, Estonia; Unidad de Endocrinología Pediátrica,†† Hospital Universitario Puerta del Mar, 11009 Cádiz, Spain; Eli Lilly and Company,§§ Indianapolis, IN 46285; and Departament de Bioquímica i Biologia Molecular,*** Universitat Autònoma de Barcelona, 08025 Barcelona, Spain

Abstract During the diagnosis of three unrelated patients with severe hypertriglyceridemia, three *APOA5* mutations [p.(Ser232_Leu235)del, p.Leu253Pro, and p.Asp332ValfsX4] were found without evidence of concomitant *LPL*, *APOC2*, or *GPIHBP1* mutations. The molecular mechanisms by which *APOA5* mutations result in severe hypertriglyceridemia remain poorly understood, and the functional impairment/s induced by these specific mutations was not obvious. Therefore, we performed a thorough structural and functional analysis that included follow-up of patients and their closest relatives, measurement of apoA-V serum concentrations, and sequencing of the *APOA5* gene in 200 nonhyperlipidemic controls. Further, we cloned, overexpressed, and purified both wild-type and mutant apoA-V variants and characterized their capacity to activate LPL. The interactions of recombinant wild-type and mutated apoA-V variants with liposomes of different composition, heparin, LRP1, sortilin, and SorLA/LR11 were also analyzed. Finally, to explore the possible structural consequences of these mutations, we developed a three-dimensional model of full-length, lipid-free human apoA-V.[JLR] A complex, wide array of impairments was found in each of the three mutants, suggesting that the specific residues affected are critical structural determinants for apoA-V function in lipoprotein metabolism and, therefore, that these *APOA5* mutations are a direct cause of hypertriglyceridemia.—Mendoza-Barberá, E., J. Julve, S. K. Nilsson, A. Lookene, J. M. Martín-Campos, R. Roig, A. M. Lechuga-Sancho, J. J. Sloan, P. Fuentes-Prior, and F. Blanco-Vaca. **Structural and functional analysis of *APOA5* mutations identified in patients with severe hypertriglyceridemia. *J. Lipid Res.* 2013.** 54: **649–661.**

Supplementary key words apoA-V • familial hyperchylomicronemia • homology modeling • molecular bases of disease • LRP1 • sortilin • SorLA/LR11 • triglyceride metabolism • type V hyperlipidemia

Hypertriglyceridemia is common in humans and is a well-established cardiovascular risk factor independent of HDL cholesterol (1). Hypertriglyceridemia is present in hyperlipidemia types I, IIb, III, IV, and V, all of which (with the exception of type I hyperlipidemia, also known as familial hyperchylomicronemia) are currently considered complex diseases with a strong polygenic component (2, 3). While *LPL* and *APOC2* gene mutations have been known for decades to be a cause of familial hyperchylomicronemia (4–6), mutations in the *APOA5* or glycosylphosphatidylinositol-anchored HDL-binding protein 1 (*GPIHBP1*) genes have been found more recently to explain some cases of this disease in which no *LPL* or *APOC2* mutations were found (7–9). *APOA5* variants have also been linked to the polygenic hyperlipidemia types IIb, III, IV, and V as well as to cardiovascular disease risk (3, 10–14).

ApoA-V was first identified and characterized as a liver preprotein of 366 amino acid residues that is secreted

This work was funded by Instituto de Salud Carlos III (ISCIII) Grants 08-1147 (to F.B.-V.), 11-01076 (to F.B.-V.), 10-00277 (to J.J.), and SAF2010-15668 (to P.F.-P.). CIBER de Diabetes and Enfermedades Metabólicas Asociadas is an ISCIII action. E.M.B. received Spanish Ministerio de Ciencia e Innovación Fellowship BES-2008-006713.

Manuscript received 12 August 2012 and in revised form 17 December 2012.

Published, JLR Papers in Press, January 10, 2013
DOI 10.1194/jlr.M031195

Abbreviations: Ch, cholesterol; DMPC, dimyristoylphosphatidylcholine; GPIHBP1, glycosylphosphatidylinositol-anchored high-density lipoprotein-binding protein 1; HSPG, heparan sulfate proteoglycan; LDLR, LDL receptor; LRP1, LDL receptor-related protein 1; PC, phosphatidylcholine; PE, phosphatidylethanolamine; PS, phosphatidylserine; RAP, receptor-associated protein; RU, resonance unit; SorLA/LR11, sorting protein-related receptor containing LDLR class A repeats; SPR, surface plasmon resonance; 3D, three-dimensional.

[1] E. Mendoza-Barberá, J. Julve, and S. K. Nilsson contributed equally to this work.

[2] To whom correspondence should be addressed.
e-mail: fblancova@santpau.cat (F.B.-V.); pfuentes@santpau.cat (P.F.-P.)

[S] The online version of this article (available at http://www.jlr.org) contains supplementary data in the form of four figures and two tables.

after removal of the signal peptide as a 343-residue protein (15, 16). (See supplementary Fig. I for a sequence alignment of mature apoA-V from different species.) In the blood, apoA-V is mainly associated with HDL and VLDL and, to a lesser extent, with chylomicrons but not with LDL (17, 18). ApoA-V plasma levels are quite low (~150 μg/l or 4 nM; for comparison, molar concentrations of apoB and apoA-I are 500- and 10,000-fold higher, respectively), which contrast with a higher liver concentration.

Despite its scarcity, a number of independent observations indicate that apoA-V is a strong modulator of serum triglycerides. An inverse relationship between apoA-V and triglyceride levels was first inferred from studies with genetically modified mice (15). However, the specific mechanism by which apoA-V reduces plasma triglycerides is unclear (19). There is in vitro and in vivo evidence that apoA-V affects plasma triglyceride metabolism through an LPL stimulatory mechanism (19). Furthermore, there are also indications for a receptor-mediated mechanism by which apoA-V could lower the serum concentration of triglyceride-rich lipoproteins. In this regard, apoA-V has been shown to interact with heparan sulfate proteoglycans (HSPG) and several lipoprotein receptors, such as the LDL receptor (LDLR), the LDL receptor-related protein 1 (LRP1), the sorting protein-related receptor containing LDLR class A repeats (SorLA/LR11), and sortilin (20–23). Whereas the roles of LDLR, LRP1, and HSPG as key factors in lipoprotein metabolism are widely accepted, the function of Vps10p-domain family members SorLA/LR11 and sortilin in lipid homeostasis remains less well understood. Interestingly, both receptors share many lipoprotein-associated ligands with LDLR family members, and they bind in particular apoE, apoA-V, LPL, and the receptor-associated protein (RAP) (21–26). Activation of LPL by apoA-V requires the enzyme to be surface-bound and a model that accounts for the role of SorLA/LR11 and sortilin in apoA-V stimulation of LPL has been recently proposed (27). Other models have also been advanced to explain the function of apoA-V in mediating receptor- or HSPG-dependent liver uptake of triglyceride-rich particles (19). Noteworthy, sortilin has been recently shown to play a role in liver VLDL secretion (reviewed in Refs. 27, 28). A third mechanism by which apoA-V may lower triglyceride levels is thought to depend on intracellular processes that reduce liver VLDL secretion and that could be linked to sortilin activity (19).

Herein, we report a thorough structural and functional analysis of three mutations found in the *APOA5* gene of three patients studied because of severe hypertriglyceridemia without concomitant *LPL, APOC2,* or *GPIHBP1* gene mutations: a 12 bp deletion, c.694_705delTCCCGGAAGCTC [p.(Ser232_Leu235)del], a c.757T>C missense mutation (p.Leu253Pro), and a 4 bp deletion, c.990_993delAACA, which results in the C-terminally truncated protein p.Asp332ValfsX4. Our results strongly suggest that the mutated residues are critical for apoA-V function in lipoprotein metabolism and therefore directly responsible for the hypertriglyceridemia found in the patients studied.

MATERIALS AND METHODS

Patients and controls

Three unrelated Spanish patients with severe hypertriglyceridemia were studied for diagnostic purposes. DNA from 200 non-hyperlipidemic subjects living in Barcelona, Spain, was used as a control (41% were women; age range: 17 to 85 years). The Ethics Committee of the Hospital de la Santa Creu i Sant Pau reviewed and approved the study protocol, and all individuals provided their written informed consent.

Plasma lipids, lipoprotein, and apo analyses

Blood samples were collected after an overnight fast. Standard, commercially available assays adapted to a Hitachi 911 autoanalyzer (Roche Diagnostics GmbH, Mannheim, Germany) were used to determine plasma total cholesterol, triglycerides, and HDL cholesterol. ApoA-V in serum was measured by ELISA as previously described (17); serum apoA-V levels in 40 normolipidemic individuals ranged from 24 to 406 μg/l, with a mean of 157 μg/l.

Gene amplification and analysis

Genomic DNA was isolated from whole blood using the QIAamp DNA blood minikit (QIAGEN, Hilden, Germany). The entire coding region of the *APOA5* gene was amplified by PCR in one fragment with the oligonucleotides 5′-ACAGGATTTCGGGCAGTTG-3′ (forward) and 5′-CAAATGAGCACTGGGAGGC-3′ (reverse). The fragment was sequenced by the Sanger method using the BigDye 3.1 sequencing kit (Applied Biosystems, Foster, CA) in an automated ABI 3130xl sequencer (Applied Biosystems). The resulting chromatograms were analyzed with the Staden package (29). To establish whether mutations p.(Ser232_Leu235)del and p.Ser19Trp identified in patient 1 were located on the same chromosome, an allele-specific PCR amplification was performed using Trp19-specific primers. The amplified fragment was then sequenced to detect the presence/absence of the p.(Ser232_Leu235)del variant.

Further, all exons and exon-intron boundaries, but not the promoter regions, of the *LPL*, *APOC2*, and *GPIHBP1* genes were also amplified and sequenced. *APOE* genotype was determined by PCR amplification and digestion with *Cfo* I as described previously (30).

Human apoA-V cloning, expression, and purification

The full-length sequence of mature human apoA-V (residues R24–P366) was cloned as a synthetic gene via nucleotide assembly; codons were optimized for expression in *Escherichia coli* while reducing the number and length of potential hairpin loops in the mRNA. The construct contains an N-terminal polyhistidine tag introduced to facilitate detection and purification of the recombinant protein, which is followed by a factor Xa cleavage site (Ile-Glu-Gly-Arg-Gly-Ala). Oligonucleotide synthesis and assembly, as well as cloning into the pET-3a vector (Novagen, Darmstadt, Germany), were performed at Entelechon GmbH (Regensburg, Germany; http://www.entelechon.com/). The sequence of the synthetic gene is available upon request.

Plasmids encoding polyhistidine-tagged mature apoA-V or its variants (see below) were transformed into *E. coli* BL21(DE3)pLysS (Stratagene, La Jolla, CA). Cells were grown at 37°C in LB medium supplemented with 100 μg/ml ampicillin and 34 μg/ml chloramphenicol to an optical density of 0.6, and then induced to express the recombinant proteins for 6 h at 20°C by adding 800 μM IPTG. After centrifugation at 4,000 *g* for 10 min, cells were lysed with B-PER supplemented with 20 mM 2-mercaptoethanol (2-ME), 1 mM EDTA, 200 mM NaCl, 10 mM $MgCl_2$, 10 mM

imidazole, 200 μg/ml lysozyme, 100 units/ml DNase I, and protease inhibitor cocktail (Sigma-Aldrich, St. Louis, MO). Recombinant proteins were subsequently purified in batch using Ni-NTA agarose beads (QIAGEN) according to the manufacturer's instructions. Briefly, bacterial extracts were diluted 1:10 (v:v) in binding buffer [25 mM sodium phosphate (pH 7.4), 200 mM NaCl, 10 mM 2-ME, 0.75 mM EDTA, 10 mM imidazole, 1% (v/v) NP-40] and incubated with the affinity matrix previously equilibrated in this solution. The matrix was thoroughly washed with binding buffer, and then three times with binding buffer containing 50 mM imidazole. Finally, specifically bound proteins were eluted with either 50 mM sodium citrate, 150 mM NaCl, 0.75 mM EDTA (pH 3.0), or with binding buffer supplemented with 500 mM imidazole. Protein concentrations were determined based on the theoretical absorption coefficients (http://web.expasy.org/protparam/).

Site-directed mutagenesis

All apoA-V mutants were generated using the QuikChange site-directed mutagenesis kit (Strategene); the primers used are given in supplementary Table I. For variant p.(Ser232_Leu235)del, we first generated an intermediate form in which the codons for residues R233 and K234 were deleted; the six nucleotides coding for residues S232 and L235 were then removed from this plasmid in a second mutagenesis step. Mutant p.Asp332ValfsX4 was generated by first inserting four thymidines after the G334-encoding triplet to generate a F335 codon followed by a TAA stop codon. This intermediate plasmid was then subjected to a second mutagenesis round to replace the wild-type D332-S333-G334 tripeptide by the mutant Val-Ala-Arg sequence.

SDS-PAGE and Western blotting

Proteins were separated on SDS-Tris-Tricine polyacrylamide gels using a Bio-Rad apparatus (Bio-Rad, Hercules, CA). Gels were either stained with Coomassie Brilliant Blue or silver, or they were transferred to PVDF membranes using a fully submerged transfer cell (Bio-Rad). For immunoblotting, membranes were blocked in TBS containing 5% skimmed milk, incubated for 1 h at room temperature with the primary antibody (mouse anti-His monoclonal antibody; GE Healthcare, Little Chalfont, UK; diluted 1:3,000), and thoroughly washed with TBS. Membranes were then similarly treated with the secondary antibody (goat anti-mouse IgG horseradish peroxidase conjugate from Pierce (Rockford, IL; 1:10,000 dilution). Blots were revealed with SuperSignal chemoluminescence system (Pierce) according to the manufacturer's instructions and exposed to autoradiography films.

Limited proteolysis

Samples of recombinant apoA-V at 100 μg/ml in 50 mM sodium citrate, 150 mM NaCl, and 0.75 mM EDTA (pH 3.0) were incubated with porcine gastric pepsin at 25°C for up to 3 h. Aliquots of the reaction were then removed and immediately mixed with Laemmli sample buffer and heated at 95°C for 10 min. Samples were separated on 12% polyacrylamide SDS-Tris-Tricine gels and either stained with Coomassie Brilliant Blue or electrophoretically transferred to PVDF membranes and probed with an anti-His antibody (see above). Alternatively, aliquots of recombinant apoA-V in 100 mM Tris-HCl, 0.1% NP-40 (pH 8.5) were incubated with sequencing-grade trypsin (100:1 ratio), and the reaction progress followed as previously mentioned.

Preparation of apoA-V-DMPC liposomes

Lipid-free apoA-V variants were complexed 1:10 w/w with dimyristoylphosphatidylcholine (DMPC) liposomes prepared by extrusion through an 0.2 μm PC filter using an Avanti Mini-Extruder and following the manufacturer's instructions (Avanti Polar Lipids, Alabaster, AL) (23). Samples were spun for 10 min at 15,000 *g* to remove residual liposomes, and protein content was determined using a BCA protein assay kit (Pierce).

ApoA-V binding to liposomes

The affinity of wild-type apoA-V and its variants for immobilized liposomes was assessed by surface plasmon resonance (31) using a Biacore 300 system (GE Healthcare). Briefly, intact liposomes of various compositions [phosphatidylcholine (PC) alone; 70% PC, 30% phosphatidylserine (PS); 40% PC, 30% PS, 30% phosphatidylethanolamine (PE); and 20% PC, 30% PS, 30% PE, 20% cholesterol (Ch), respectively] were noncovalently immobilized on L1 sensor chips (Biacore, Uppsala, Sweden) following the procedure described elsewhere (32, 33). Nonspecific binding sites were blocked with 0.1 mg/ml BSA (BSA). All binding experiments were carried out at 25°C in 20 mM HEPES, 0.15 M NaCl (pH 7.4). Analytes were injected at a flow rate of 30 μl/min, and sensorgrams were recorded and analyzed using BIAevaluation 4.1 software. The sensor chip surface was regenerated after each binding experiment by the injection of 50 mM NaOH, 50% isopropanol, and 0.01% CHAPS.

ApoA-V binding to heparin

The affinity of wild-type apoA-V and its variants for immobilized heparin was assessed by surface plasmon resonance (SPR). Streptavidin was first immobilized on CM5 sensor chips (Biacore) using the amine coupling kit and following the manufacturer's instructions. The amount of immobilized streptavidin varied between 3,500–4,000 resonance units (RU). Next, 180–200 RU of biotinylated heparin (Sigma) was coupled to these streptavidin-coated sensor chips via the covalently bound streptavidin moiety. Analytes (apoA-V variants) were injected at a flow rate of 30 μl/min, and sensorgrams were recorded and analyzed using BIAevaluation 4.1 software.

ApoA-V interaction with LRP1 clusters II and IV

Recombinant human apoA-V variants were biotinylated using the sulfhydryl-reactive EZ-Link Biotin-BMCC (Thermo Scientific, Rockford, IL) following the manufacturer's instructions. The maleimide reactive group of this compound selectively reacts with the single cysteine residue in the apoA-V primary sequence, C227. For biotinylation, proteins were previously dialyzed into PBS (pH 6.5) using 0.5-ml Zeba Desalt Spin Columns (Thermo Scientific) to optimize formation of a stable thioether bond with the maleimide moiety. Successful derivatization was verified by separating the reaction products on a 10% SDS-polyacrylamide gel, followed by electroblotting onto a nitrocellulose membrane. The membrane was blocked with Odyssey blocking buffer diluted in PBS (pH 7.4) and incubated with IRDye 800CW streptavidin (LI-COR Biosciences, Lincoln, NE) in Odyssey blocking buffer diluted in PBS (pH 7.4), 0.1% Tween 20, and finally visualized with an Odyssey imager.

For ligand blotting, 2.5 μg of recombinant human LRP1 cluster II Fc chimera (R and D Systems, Minneapolis, MN) and cluster IV Fc chimera (R and D Systems) were separately run on a 10% SDS-polyacrylamide gel under nonreducing conditions, and then blotted onto a nitrocellulose membrane. Nitrocellulose strips containing LRP1 clusters II or IV were extensively rinsed with PBS (pH 7.4) containing 2 mM $CaCl_2$, and blocked with Odyssey blocking buffer diluted in the previously mentioned buffer (1:1, v:v) at room temperature for 30 min. Strips were then incubated with the biotinylated, recombinant wild-type human apoA-V or its mutants at a final concentration of 5 μg/ml in diluted blocking buffer at 4°C overnight with continuous shaking.

Next, the strips were rinsed with PBS (pH 7.4), 0.1% Tween-20, and 2 mM $CaCl_2$, and then incubated and visualized as explained above.

ApoA-V binding to sortilin and SorLA/LR11

Soluble receptors used for SPR were prepared and coupled to CM5 sensor chips as previously described (22, 23), and functionality of immobilized receptors was confirmed with the well-known pan-ligand RAP. Owing to the complex binding behavior of apoA-V and the inability to regenerate flow cells injected with the apolipoprotein, conventional kinetic studies cannot be performed in this system. Therefore, we used single-cycle kinetics, which has proved suitable for kinetic analysis when cell regeneration is not possible (34). Further, considering that apoA-V is found in plasma only as a lipid-associated protein and to mimic triglyceride-rich lipoproteins, apoA-V incorporated into 0.2-μm DMPC liposomes was employed for these studies.

ApoA-V-DMPC liposomes were injected in five sequential steps of increasing concentration over flow cells containing immobilized receptors; a flow cell with an equivalent amount of immobilized BSA was used as reference. Injections were set to last 60 s with a corresponding dissociation phase of 184 s at a continuous flow of 30 μl/min. After the last injection, a dissociation phase of 20 min was added. Binding to the reference flow cell was subtracted from the active cell, and the data were further adjusted for instrument noise and complete double referencing with a buffer-only injection cycle. Kinetics parameters (association and dissociation rate constants) were determined using BIAevaluation 4.1 software by assuming a 1:1 binding model, from which the equilibrium dissociation constants K_D were calculated. Protein-free liposomes were shown not to interact with the immobilized receptors by themselves.

In vitro hydrolysis of triolein liposomes by HSPG-bound LPL

A previously reported assay (35) with minor modifications was used to determine the hydrolysis rate of triolein-based liposomes by HSPG-bound LPL. To prepare the lipid emulsion, 1.2 μl/well of a concentrated stock emulsion of 34.7 mM triolein and 17.8 mM glycerol tri[9,10(n)-^{3}H]oleate (5 mCi/ml and 21 Ci/mmol, respectively; purchased from PerkinElmer, Waltham, MA) were taken. The solvent was removed and the lipid emulsion formed by vigorous sonication in 28.9 mM Pipes (pH 7.5) containing 57.4 mM $MgCl_2$ and 0.5% (w/v) fatty acid-free BSA (Sigma). The lipid emulsion was associated for 30 min at 37°C with the different recombinant apoA-V variants (10 μg/ml) and with 1 μM human apoC-II.

A 96-well microtiter plate was incubated with 100 μl/well of a 5 μg/ml solution of HSPG in PBS (pH 7.4) for 18 h at 4°C (Sigma). After washing with PBS, the wells were blocked with PBS containing 1% fatty acid-free BSA at 37°C for 1 h. Bovine LPL, prepared according to Ref. 36 in 0.1 M Tris·HCl (pH 8.5) and 20% glycerol, was then added to the wells (100 μl/well at 5 μg/ml) and incubated at 4°C for 1 h. The microtiter plate was finally washed again with 0.1 M Tris (pH 8.5). Lipolysis was started by the addition of apoA-V-liposome complexes to the HSPG-LPL-containing plates and stopped after 30 min with Triton X-100 (1% final concentration). Fifty microliters from each well were transferred to glass tubes, and FFA was extracted from nonhydrolyzed triglycerides by adding 1.2 ml of chloroform:methanol:n-heptane (1.45:1.21:1, v:v:v) and 0.33 ml borate-carbonate buffer [0.1 M H_3BO_3 and 0.1 M K_2CO_3 (pH 10.5)]. Each tube was thoroughly mixed and centrifuged at 2,000 rpm at 4°C for 10 min. The radiolabeled FFA fraction in the supernatant was counted in a 1500 Packard Tri-Carb β counter (PerkinElmer).

Bioinformatics analysis

For automated modeling, the amino acid sequence of the mature human apoA-V was submitted to various modeling servers through the Protein Modeling Portal (http://www.proteinmodelportal.org/). The sequence was also independently submitted to servers 3D-JIGSAW (http://bmm.cancerresearchuk.org/~3djigsaw/) and Geno3D (http://geno3d-pbil.ibcp.fr/). Protein structures were displayed and analyzed using the molecular graphics program MIFit (http://code.google.com/p/mifit/), and figures were prepared with PyMOL (http://www.pymol.org/). The impact of point mutations on the structure and function of the protein were assessed with PolyPhen (http://genetics.bwh.harvard.edu/pph/), SIFT (http://sift.bii.a-star.edu.sg/), CUPSAT (http://cupsat.tu-bs.de/), I-Mutant2.0 (http://folding.uib.es/i-mutant/i-mutant2.0.html), and PoPMuSiC (http://babylone.ulb.ac.be/popmusic/).

RESULTS

Patients: clinical and family data, serum apoA-V levels, and mutation analysis

Samples from three unrelated patients were referred (to F.B.-V.) for the molecular study of severe hypertriglyceridemia. None of them were overweight or suffered from diabetes mellitus, and the only adult, patient 1, consumed almost negligible amounts of alcohol. Genetic analysis of patient 1 was requested after fibrate treatment failed to reduce the severe hypertriglyceridemia (see **Table 1** for a summary of the main clinical and biochemical data). The patient, however, did not return to the hospital for follow-up until years later, when he attended the Emergency Unit because of abdominal pain and was diagnosed of acute pancreatitis. Over the years, patient 1 has been treated with different fibrates and ω-3 fatty acids, but he only occasionally presented a normalized lipid profile. However, his long-term compliance with the treatment regime cannot be ensured. The severe hypertriglyceridemia of patient 2 was discovered in a routine blood analysis requested during the study of a granuloma annulare. The girl was of South American origin, and her mother did not suffer from hyperlipidemia; no other family history or clinical follow-up information is available. Patient 3 presented with tuberous xanthomas, which led to the diagnosis of severe hypertriglyceridemia. A history of hyperlipidemia without clinical cardiovascular disease was known in the father's family of this patient (see supplementary Fig. II for more family details). After diagnosis, relatively good clinical control of the hypertriglyceridemia was achieved with ω-3 fatty acids, and in a recent blood analysis, serum triglycerides and cholesterol concentrations were 3.1 and 4.4 mmol/l, respectively.

In the three cases, *APOA5* mutations were found without concomitant mutation in the *LPL*, *APOC2*, or *GPIHBP1* gene (see Table 1 for a summary of the main genetic data). None of the *APOA5* mutations found in the patients were identified in 200 nonhyperlipidemic control individuals living in Barcelona, Spain. A common *APOA5* polymorphism (rs3135506, p.Ser19Trp) repeatedly linked to hypertriglyceridemia (3, 10, 11, 37) was found in heterozygosis

TABLE 1. Main clinical, biochemical, and genetic information for the three patients studied

	Patient 1	Patient 2	Patient 3
Age	44	5	4
Gender	Male	Female	Female
Clinical signs typically associated with severe hypertriglyceridemia	None	None	Tuberous xanthoma
Triglycerides (mmol/l; recommended < 1.7)	22	15.3	19.9
Cholesterol (mmol/l; recommended < 5)	6.8	5.2	16.2
HDL cholesterol (mmol/l; recommended > 1)	0.7	0.5	0.7
APOE genotype	E3/E3	E3/E3	E3/E2
Mutations in *LPL*, *APOCII*, or *GPIHBP1* genes	No	No	No
APOA5 mutations	c.694_705delTCCCGGAAGCTC (p.Ser232_Leu235) in heterozygosis	c.757T>C (p.Leu253Pro) in homozygosis	Compound heterozygosis for c.289C>T (p.Gln97×) and c.990_993delAACA (p.Asp332ValfsX4)
APOA5 SNP *rs3135506* or *rs651821*	rs3135506 (p.Ser19Trp) in heterozygosis[a]	No	No
ApoA-V serum concentration[b]	375 μg/L	145 μg/l	ND[c]
Family history available?	No	Mother without hypertriglyceridemia	Yes (see supplementary Fig. II)

[a] SNP rs3135506 is within the wild-type allele.
[b] Range in normolipidemic individuals: 24-406 μg/l (17).
[c] Not determined in the initial study. In a later determination, serum apoA-V concentration was 535 μg/l, while her plasma triglyceride levels had dropped to about 25% of the initial value.

in patient 1, being present in the wild-type allele. Neither this nor another common *APOA5* polymorphisms previously linked to hypertriglyceridemia (rs651821) were present in the other patients studied.

Cloning, expression, and characterization of recombinant human apoA-V

To experimentally determine the underlying molecular defect(s) leading to hypertriglyceridemia in our patients, we overexpressed full-length, mature human apoA-V as well as the three novel apoA-V mutants detected [p.(Ser232_Leu235)del, p.Leu253Pro, and p.Asp332ValfsX4]. Both wild-type, recombinant human apoA-V, and the three mutants were straightforwardly purified by metal affinity chromatography (supplementary Fig. III). Their identities were verified by Western blot and mass spectrometry analysis of trypsin digests (supplementary Table II).

For the envisioned functional studies, it was critical to employ properly folded proteins. Of note, most of the recombinant human apoA-V was recovered from the cytosolic, soluble fraction of *E. coli* cultures (supplementary Fig. III), which strongly suggests that it was correctly folded. However, and to verify this point while avoiding protein aggregation, we subjected wild-type apoA-V to limited proteolysis with pepsin at acidic pH, similar to a recent report (see Materials and Methods and Ref. 38). As shown in supplementary Fig. IV-A, the recombinant protein was rapidly cleaved to generate a transient ~30 kDa fragment, which was converted into a stable ~20 kDa form after 30 min incubation with the protease. Importantly, this fragment appeared to be fully resistant to further pepsinolysis for at least 3 h. The preferential cleavage of just two scissile peptide bonds out of the 74 sites predicted for a fully unfolded protein (http://web.expasy.org/peptide_cutter/), and generation of a stable "core" fragment of apoA-V strongly suggests that the recombinant protein was properly folded. Similar results were obtained when apoA-V samples were treated with trypsin at basic pH, in the presence of detergent NP-40 added to guarantee solubility at this pH value (supplementary Fig. IV-B).

During the overexpression experiments of mutant p.Leu253Pro, the presence of a major degradation form with an apparent M_r ~33 kDa was repeatedly observed (supplementary Fig. III, lanes 5, 6). This truncated form was not observed when either wild-type apoA-V or the other two mutants were expressed, and presumably it resulted from the action of an endogenous proteinase(s). Of note, an apparently more radical protein modification, such as truncation of the last C-terminal residues in mutant p.Asp332ValfsX4, did not enhance protease sensitivity (supplementary Fig. III, lanes 7, 8). To verify that the introduced mutations did not result in an overall destabilization of the protein structure, limited proteolysis experiments were performed with the purified mutant proteins, as described above for wild-type apoA-V. In all three cases, a similar cleavage pattern was observed, characterized by the formation of a stable N-terminal fragment resistant to further proteolysis for at least 3 h (data not shown). The major degradation form of apoA-V mutant p.Leu253Pro was recognized by anti-His antibodies (data not shown), indicating that the mutant protein was cleaved within its C-terminal region. Comparison of the distances migrated by various apoA-V variants and proteolytic products (supplementary Figs. III and IV) indicated that cleavage occurred downstream of the A260–F261 peptide bond, most likely between residues 300 and 310. These observations suggest that the Leu253→Pro replacement induces long-range structural changes, which specifically affect the C-terminal apoA-V region.

Impaired liposome binding by apoA-V mutant p.Leu253Pro

Once it was demonstrated that recombinant apoA-V variants were properly folded, we started the analysis of their

interactions with various biomolecules. Lipid binding properties of wild-type and apoA-V mutants were examined using four different types of liposomes. At low apoA-V concentrations, the curves followed simple 1:1 binding kinetics. Sensorgrams demonstrating binding of wild-type and mutant apoA-V variants to immobilized liposomes are presented in **Fig. 1**. Calculated kinetic constants are given in **Table 2**. As can be seen, all apoA-V mutants bound to these liposomes with high affinity; the K_d values varied between 0.1 and 18.6 nM. The liposome composition did not significantly influence binding parameters, but the affinity for PC-PS-based liposomes was in general higher than for other liposome compositions. Interestingly, mutants p.Asp332ValfsX4 and p.(Ser232_Leu235)del bound somewhat more tightly to liposomes than the wild-type protein (2–12 times lower K_d values). The association rate constants of these mutants were comparable to the corresponding values of wild-type apoA-V; however, their higher affinity for liposomes was the result of slower dissociation. In comparison with other studied variants, a significantly lower affinity was detected for the mutant p.Leu253Pro, mainly caused by a relatively fast dissociation from the immobilized liposomes (Fig. 1D and Table 2).

Mutants p.(Ser232_Leu235)del and p.Asp332ValfsX4 show impaired binding to immobilized heparin

Next, and considering that HSPG has been reported to be a bona fide apoA-V receptor, we compared the affinity of wild-type apoA-V and the mutants to immobilized heparin via SPR. Although all apoA-V variants interacted with streptavidin-bound biotinylated heparin, their kinetic parameters varied considerably; wild-type apoA-V and the point mutant p.Leu253Pro bound to heparin with similar affinity, whereas the deletion mutants p.(Ser232_Leu235)del and p.Asp332ValfsX4 had somewhat lower affinity (**Fig. 2**). This difference was mainly due to slower association, as the dissociation rate constants of the proteins were of the same order of magnitude.

ApoA-V interaction with LRP1 clusters II and IV

ApoA-V is known to be internalized via classical lipoprotein receptors of the LDLR family, including LRP1 and SorLA/LR11 (22). To test whether the identified apoA-V mutants could be compromised in terms of receptor binding and internalization and to define interacting domains within LRP1, we analyzed the capacity of the recombinant variants to bind two major functional units of the receptor, termed clusters II (residues R786–L1165 of the full-length human receptor) and IV (S3332–D3779). Wild-type apoA-V and the three mutants bound to membrane-immobilized LRP1 cluster II to an apparently similar extent when adjusted for apoA-V concentration (**Fig. 3**). By contrast, no interaction with wild-type apoA-V or the mutant apoA-V forms was observed when the cluster IV of LRP1 was used instead (data not shown).

Defective sortilin and SorLA/LR11 interactions with apoA-V mutants

Failure to detect differences in LRP1 binding by wild-type and mutant apoA-V prompted us to focus on the interactions with two other physiologic receptors: sortilin and SorLA/LR11. The results of our SPR analysis of

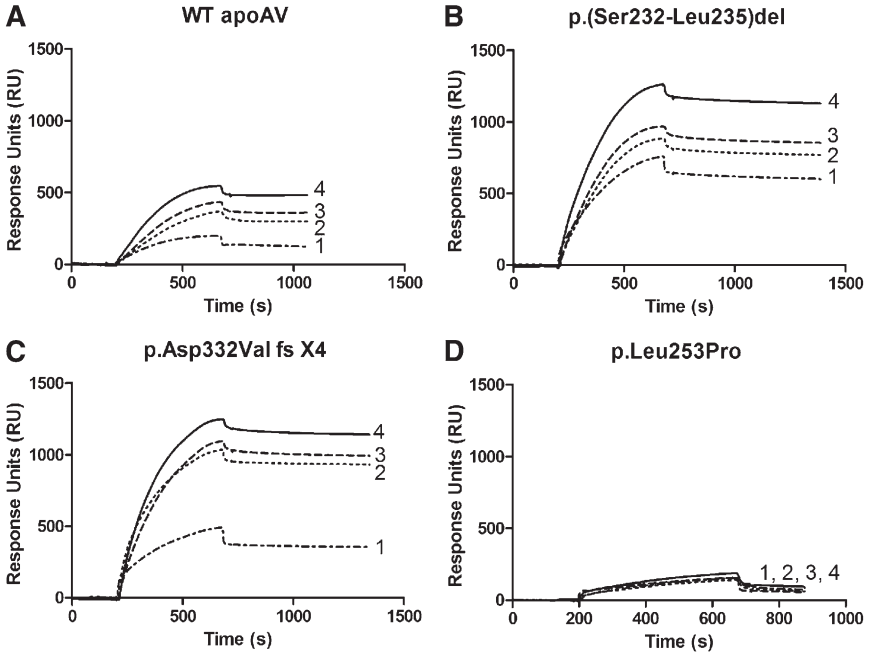

Fig. 1. Binding of apoA-V mutants to intact liposomes. The lipid-binding ability of wild-type apoA-V (A) and variants p.(Ser232_Leu235)del (B), p.Asp332ValfsX4 (C), and p.Leu253Pro (D) was examined by surface plasmon resonance using four different types of liposomes immobilized on L1 chips. Liposome compositions were as follows: (1) 100% PC; (2) 70% PC, 30% PS; (3) 40% PC, 30% PS, 30% PE; and (4) 20% PC, 30% PS, 30% PE, 20% Ch. Sensorgrams shown are representative of SPR experiments performed four times with similar results and evaluated with BIAevaluation 4.1 software (see Materials and Methods for details).

TABLE 2. Kinetic parameters of the binding of recombinant human apoA-V and its mutants to intact L1-immobilized liposomes

Liposome	k_{ass} ($M^{-1}s^{-1}$)	k_{diss} (s^{-1})	K_D (nM)
Wild-type apoA-V			
PC	1.4×10^5	1.3×10^{-4}	0.9
PC-PS	1.3×10^5	1.3×10^{-4}	1.0
PC-PS-PE	1.2×10^5	4.4×10^{-4}	3.7
PC-PS-PE-Ch	1.3×10^5	4.2×10^{-4}	3.2
p.(Ser232_Leu235)del			
PC	1.3×10^5	6.0×10^{-5}	0.5
PC-PS	1.6×10^5	2.3×10^{-5}	0.1
PC-PS-PE	1.5×10^5	4.4×10^{-5}	0.3
PC-PS-PE-Ch	2.3×10^5	4.2×10^{-5}	0.2
p.Asp332ValfsX4			
PC	1.7×10^5	8.5×10^{-5}	0.5
PC-PS	2.2×10^5	4.8×10^{-5}	0.2
PC-PS-PE	2.1×10^5	6.3×10^{-5}	0.3
PC-PS-PE-Ch	2.3×10^5	6.4×10^{-5}	0.3
p.Leu253Pro			
PC	0.7×10^5	8.1×10^{-4}	11.6
PC-PS	0.9×10^5	6.6×10^{-4}	7.3
PC-PS-PE	0.7×10^5	1.30×10^{-3}	18.6
PC-PS-PE-Ch	0.8×10^5	1.31×10^{-3}	16.4

Kinetic constants were calculated using BIAevaluation 4.1 software.

apoA-V interactions with sortilin covalently bound to CM5 sensor chips are shown in **Fig. 4**. Wild-type apoA-V-DMPC liposomes interacted with sortilin with high affinity (in the mid-picomolar range; Fig. 4A). Mutants p.(Ser232_Leu235)del and p.Asp332ValfsX4 showed a somewhat defective sortilin interaction, displaying approximately 4- and 1.7-fold higher K_D values than wild-type apoA-V, respectively (Fig. 4B, C). Unexpectedly, the mutant p.Leu253Pro

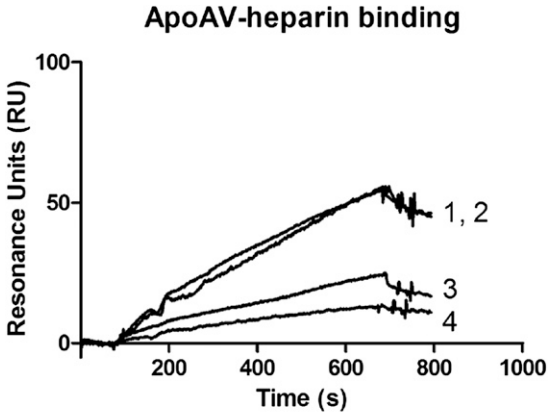

ApoAV variant	k_{ass} ($M^{-1}s^{-1}$)	k_{diss} (s^{-1})	K_d (nM)
1. WT apoAV	$2.9x10^4$	$7.6x10^{-4}$	2.6
2. p.Leu253Pro	$2.3x10^4$	$8.9x10^{-4}$	3.9
3. p.Asp332Val fs X4	$0.3x10^4$	$6.4x10^{-4}$	21.3
4. p.(Ser232-Leu235)del	$0.6x10^4$	$6.3x10^{-4}$	10.5

Fig. 2. Heparin-binding properties of apoA-V mutants. ApoA-V binding to heparin was examined by surface plasmon resonance. For these experiments, biotinylated heparin was coupled to CM5 sensor chips via covalently immobilized streptavidin. Sensorgrams shown are representative of SPR experiments repeated twice with similar results and were evaluated with BIAevaluation 4.1 software (see Materials and Methods for details). Kinetic parameters for wild-type (1) and mutant apoA-V variants (2–4) are given below the sensorgrams.

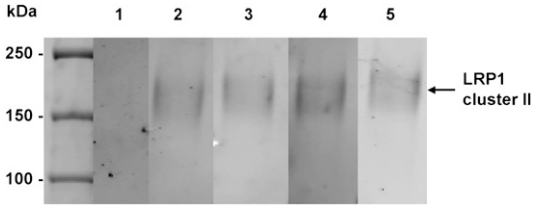

Fig. 3. Ligand blot analysis of apoA-V binding to LRP-1 cluster II. Samples of recombinant LRP1 cluster II were separated under nonreducing conditions on a 10% SDS-polyacrylamide gel and electrophoretically transferred onto a nitrocellulose membrane. Strips containing equal amounts of the LRP1 cluster were incubated in the absence (lane 1) or presence of biotinylated, recombinant human wild-type apoA-V (lane 2), p.(Ser232_Leu235)del (lane 3), p.Asp332ValfsX4 (lane 4), and p.Leu253Pro (lane 5). Bound proteins were revealed with IRDye 800CW Streptavidin and visualized with an Odyssey Imager.

did not show any appreciable interaction with sortilin (Fig. 4D).

Finally, we analyzed apoA-V interactions with another multifunctional endocytic receptor, SorLA/LR11. As demonstrated above for sortilin, wild-type apoA-V bound tightly to the immobilized receptor (**Fig. 5A**), whereas mutant p.Leu253Pro was found to be devoid of SorLA/LR11-binding ability (Fig. 5D). Interestingly, mutant p.(Ser232_Leu235)del also displayed a complete SorLA/LR11 binding deficiency (Fig. 5B), indicating fundamentally different mechanisms of apoA-V interaction with sortilin and SorLA. The deletion mutant p.Asp332ValfsX4 showed measurable but largely impaired binding to SorLA/LR11 compared with wild-type apoA-V (80-fold lower K_D value; Fig. 5C). This deficiency was mainly explained by a very high dissociation rate constant.

ApoA-V stimulation of LPL activity

As mentioned previously, current evidence supports the view that apoA-V affects plasma triglyceride levels at least partly through LPL activity stimulation. To verify whether some of the apoA-V mutants could differ in the extent of LPL stimulation, we analyzed the impact of wild-type and mutant apoA-V forms on the activity of HSPG-bound LPL. The fold changes relative to LPL alone were as follows: wild-type apoA-V, 1.3-fold ($P < 0.001$); p.(Ser232_Leu235)del, 1.1-fold (NS); p.Asp332ValfsX4, 1.4-fold ($P < 0.001$); p.Leu253Pro, 0.02-fold ($P < 0.001$); and wild-type apoA-V + bovine apoCIII (positive control of LPL inhibition), 0.6-fold ($P < 0.001$) (**Fig. 6**; values > 1.0 indicate increases, values < 1.0 decreases in LPL activity). Thus, rather than stimulate LPL activity, mutant p.Leu253Pro actually behaved as a potent inhibitor of triglyceride hydrolysis.

A three-dimensional model for human apoA-V can be generated based on its homology to apoA-I

The results of limited proteolysis experiments performed by us and others (see above and Ref. 38) suggested a domain organization for lipid-free apoA-V analogous to that previously determined for apoA-I (39) and apoE (40). Thus, in the absence of lipids, apoA-V would be expected to feature an elongated, four-helix bundle comprising

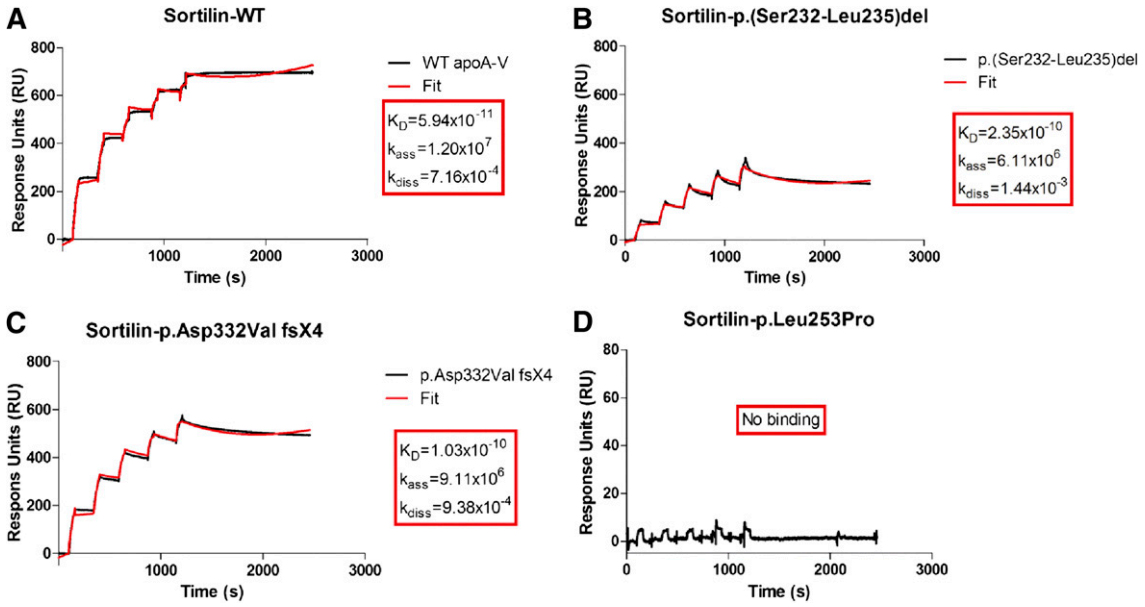

Fig. 4. Binding of apoA-V-DMPC variants to sortilin studied by surface plasmon resonance. Sortilin was covalently immobilized to CM5 sensor chips. Wild-type apoA-V (A) and variants p.(Ser232_Leu235)del (B), p.Asp332ValfsX4 (C), and p.Leu253Pro (D) complexed with DPMC were injected at increasing concentrations (16, 32, 64, 128, and 256 nM) over sortilin-coated and reference flow cells. Data shown were corrected by the signal from the reference flow cell and by a buffer-only injection cycle. When applicable, association and dissociation rate constants as well as calculated equilibrium dissociation constants are given in the corresponding panel (k_{ass}, $M^{-1}s^{-1}$; k_{diss}, s^{-1}; K_D, M). Black curves represent experimental data, and red curves represent the fit of the data to a kinetic titration 1:1 interaction model. The experiment was performed twice with similar results.

N-terminal residues R24 to about L198, followed by a loosely attached double-helical segment (residues H205 to about A260) (**Fig. 7A**). Finally, the C-terminal stretch up to P366 appears to be essentially disordered in the absence of lipids, but it quickly adopts a helical conformation upon phospholipid binding (41). The significant sequence similarity between human apoA-I and apoA-V (supplementary Fig. I) suggested the crystal structure of the former as an appropriate template for developing a three-dimensional (3D) model of the N-terminal residues R24–A260 of human apoA-V via homology modeling. Indeed, about 100 of these residues are identical or physicochemically similar in the two apolipoproteins.

However, closer inspection revealed that most of the apoA-I residues that form an almost continuous aromatic core for its N-terminal four-helix bundle (e.g., Y29, F33, F71, F104, W108, Y115) are replaced by others with less bulky, aliphatic side chains in apoA-V (supplementary Fig. I). Therefore, and to generate unbiased models of human apoA-V, we submitted the sequence of the mature apolipoprotein to various independent modeling servers. In line with the sequence similarity discussed above, one of the top models generated by I-TASSER closely followed the apoA-I architecture for helices A–F (Fig. 7B). In addition, this model featured two C-terminal α-helices that could not be modeled based on the apoA-I template. In particular, the predicted C-terminal helix H comprises residues P326 to H360, fully in line with available experimental data (41) and secondary structure predictions. Models yielded by other servers also featured all α-helical bundles that could be partially superimposed on the apoA-I-derived model.

DISCUSSION

We report an in-depth analysis of three unrelated Spanish patients who presented severe hypertriglyceridemia. Since no mutations were found in the coding regions of their *LPL*, *APOC2*, or *GPIHBP1* gene, we turned our attention to another gene, *APOA5*, which has been associated with this condition since its discovery (15). In patient 1, an adult at the time of diagnosis, a novel *APOA5* mutation p.(Ser232_Leu235)del and the common polymorphism p.Ser19Trp in the wild-type allele were identified. Apparently, other unknown genetic or environmental factor(s) contributed to his predisposition to severe hypertriglyceridemia. In this regard, not all heterozygous individuals with truncated apoA-V present with severe hypertriglyceridemia, especially in the absence of other risk factors, such as diabetes mellitus (7, 8). On the other hand, current genetic and clinical information suggests that cases 2 and 3 suffer from familial hyperchylomicronemia, as the patients were children with mutations in both alleles of the *APOA5* gene (homozygous p.Leu253Pro mutation and p.Gln97× / p.Asp332ValfsX4 mutations, respectively). Patient 3, however, showed high serum cholesterol levels, which is unusual in familial hyperchylomicronemia. It is currently unknown whether this is due to increased remnant lipoproteins and could relate to the presence of an *APOE2* allele in the setting of a severe hypertriglyceridemia. To the best of our knowledge, only one case of familial hyperchylomicronemia due to an *APOA5* homozygous mutation had been described before (7).

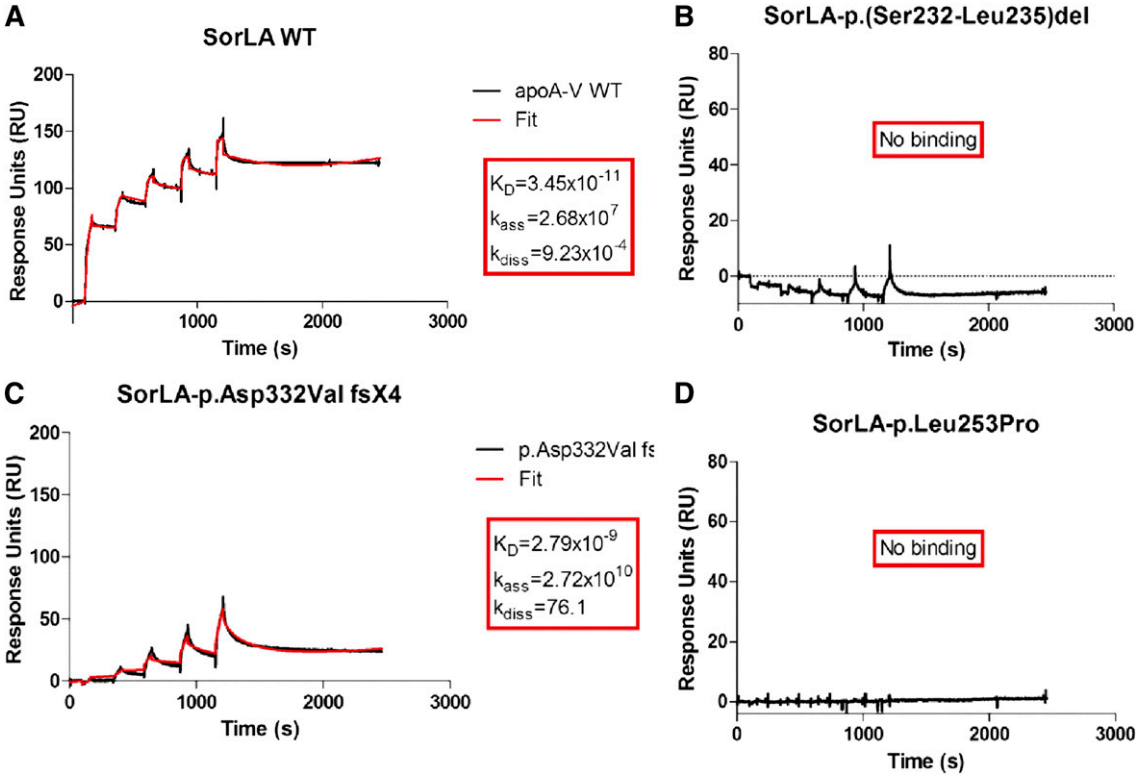

Fig. 5. Binding of apoA-V-DMPC variants to SorLA/LR11 studied by surface plasmon resonance. SorLA/LR11 was covalently immobilized to CM5 sensor chips, and experiments were performed under the same conditions as indicated in Fig. 4 legend. Data shown were corrected by the signal from the reference flow cell and by a buffer-only injection cycle. When applicable, association and dissociation rate constants as well as calculated equilibrium dissociation constants are displayed in the corresponding panel (k_{ass}, $M^{-1}s^{-1}$; k_{diss}, s^{-1}; K_D, M). Black curves represent experimental data, and red curves represent the fit of the data to a kinetic titration 1:1 interaction model. The experiment was performed twice with similar results.

The molecular mechanisms that result in severe hypertriglyceridemia in patients with *APOA5* mutations remain poorly understood, and only one study to date has addressed the capacity of apoA-V mutants to interact with LDLR family members and activate LPL (42). In addition, a recent report focused on the role of residue G185 in apoA-V-mediated LPL stimulation (43). Therefore, we performed functional analyses of the three novel *APOA5* mutations that do not have an obvious impact on apoA-V function. The results of these studies are summarized in **Table 3** and discussed below.

First, we notice that apoA-V was detected by ELISA in the serum of all three patients. In fact, the serum apoA-V concentrations of patients 1 and 2 would be at the 95th percentile and in the mean of a normolipidemic control group. In line with these findings, similar amounts of both wild-type apoA-V and all three mutants could be produced as properly folded proteins by recombinant expression in *E. coli* cells. A lack of correlation between serum apoA-V and triglyceride levels in patients with hypertriglyceridemia without extreme apoA-V deficiency has been previously described and discussed (19, 44, 45). Possibly, the excess of serum triglyceride-rich particles compensates for a decrease in the synthesis or secretion of apoA-V, provided the mutation does not cause an extreme protein deficiency.

While our study was in progress, mutant p.Leu253Pro was found in heterozygosis in an Italian patient with severe hypertriglyceridemia (46). We did not find this mutation in 200 Spanish control individuals; neither was it found in 350 subjects randomly selected from an Italian population (46). It is thus likely that this *APOA5* mutation is causally linked to the observed phenotype, especially considering that residue L253 is strictly conserved from amphibians to humans. In fact, this apparently less deleterious point mutation, compared with both the internal [p.(Ser232_Leu235)del] and C-terminal (p.Asp332ValfsX4) deletions, presented the most notable molecular defects, including higher sensitivity to proteolysis and impaired interactions with immobilized liposomes. Further, the p.Leu253Pro mutant was fully defective in terms of sortilin and SorLA/LR11binding, and it failed to stimulate LPL activity. In contrast, this variant retains the capacity to interact with LRP1 cluster II, and it binds to heparin with similar affinity as the wild-type protein.

In line with the strict conservation of L253, PolyPhen classifies the Leu253→Pro mutation as "probably damaging," and SIFT as "not tolerated." For comparison, the apoA-V polymorphism p.Ala315Val, which is associated with normal plasma TG levels (47), is classified as "benign" or "tolerated." I-Mutant2.0 also predicts decreased stability for this mutant ($\Delta\Delta G = -0.67$ kcal/mol), in contrast to an increase of almost the same magnitude for the p.Ala315-Val variant. Residue L253 is essentially buried at the interface between helices E and F in the 3D model of human

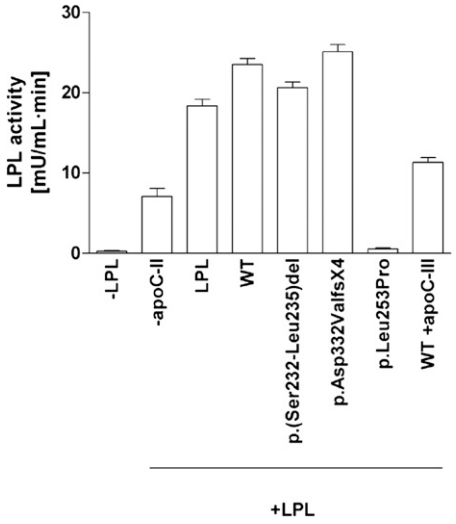

Fig. 6. Effect of wild-type and mutant apoA-V variants on triglyceride hydrolysis by HSPG-bound LPL. A triolein-based, tritium-labeled lipid emulsion was incubated with recombinant wild-type apoA-V or the three studied apoA-V mutants (10 μg/ml) at 37°C for 30 min. Next, the liposome-protein complexes were incubated for 30 min with 5 μg/ml LPL immobilized on HSPG, and the radiolabeled FFA fraction in the supernatant was measured. The results shown are the mean of experiments performed seven times; in each experiment, samples were determined in duplicate. One milliunit of lipolytic activity represents the release of 1 nmol fatty acid/min. Lane 1, –LPL: no LPL was added; lane 2, –apoC-II: LPL but no apoC-II was added; lane 3, LPL: LPL and apoC-II were added; lane 4, WT: LPL, apoC-II, and wild-type apoA-V were added; lane 5, p.(S232_L235)del: LPL, apoC-II, and p.(Ser232_Leu235)del apoA-V were added; lane 6, p.D332VfsX4: LPL, apoC-II, and p.Asp332ValfsX4 apoA-V were added; lane 7, p.L253P: LPL, apoC-II, and p.Leu253Pro apoA-V were added; lane 8, WT + apoC-III: LPL, apoC-II, apoC-III, and wild-type apoA-V were added.

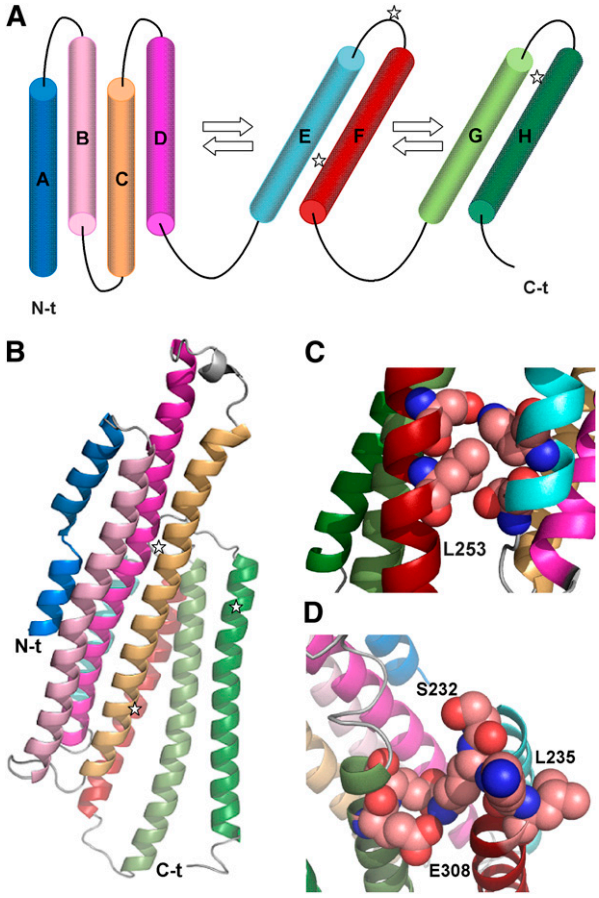

Fig. 7. Hypothetical structure of lipid-free/lipid-poor human apoA-V. (A) Schematic representation of the predicted helix arrangement in human apoA-V. Similar to the related apoA-I and apoE, the four N-terminal helices (A–D) are predicted to form a stable bundle that interacts weakly with the pair of following helices (E and F). Finally, the C-terminal residues appear to be poorly ordered in the free apolipoprotein but become rapidly folded into a further pair of helices (G and H) in the presence of lipids. (B) Three-dimensional model of apoA-V. Similar to the crystal structure of human apoA-I, the four N-terminal α-helices (A–D) are arranged in an up-and-down topology, and are followed by a pair of helices (E and F) that make only limited contacts with the major bundle. The model predicts that the C-terminal residues of apoA-V fold into an additional pair of helices (G and H), which form a continuous layer with the preceding E-F pair but which lack significant contacts with the N-terminal four-helix bundle. The positions of studied mutations are highlighted in (A) and (B). (C) Close-up of the 3D model around residue L253. Notice that the leucine side chain is buried at the interface between helices E and F, where its main chain N and O atoms engage in hydrogen bonding with other residues of helix F, explaining the deleterious impact of the Leu253→Pro exchange. (D) Close-up around the E-F loop (residues S232–L235). Notice that the side chain of residue R233 is clamped between the carboxylates of two well-conserved acidic residues donated by helix G, E308 and E309. In (C) and (D), selected residues are shown as color-coded Van-der-Waals spheres.

apoA-V (Fig. 7C). Therefore, its replacement by a proline would have a double impact on the protein structure: loss of hydrogen bond interactions to residue L250 and perhaps also L257, and creation of a small cavity at this interface. Considering similar structural rearrangements for apoA-V such as those well-documented for apoA-I (39, 48–51), it is conceivable that local unfolding around position 253 leads to the sequential "melting" of helices F and E, which perhaps propagates to the downstream helices. In line with these qualitative considerations and based on the homology model, CUPSAT predicted the Leu253→Pro replacement to be both unfavorable and destabilizing with a $\Delta\Delta G$ value of −0.69 kcal/mol, and PoPMuSiC classified the mutation as destabilizing due to an even larger drop in free energy. It is interesting to note that the nearby, also strictly conserved L242 was found replaced by a proline in a hyperchylomicronemic proband; however, its causal involvement in the disease was not established (52). In the light of our current findings, it is likely that also in this case the disease phenotype was directly related to the *APOA5* point mutation. Conceivably, these nonconservative leucine-to-proline replacements would affect the protein structure in the lipid-free/lipid-poor conformation, resulting in a higher susceptibility to proteolysis. On the other hand, the absence of these hydrophobic side chains would compromise phospholipid binding, as demonstrated here for the p.Leu253Pro variant.

The effects of apoA-V mutants on LPL activation appear to be highly variable depending on the affected residue (7, 8, 42, 43). However, it is noteworthy that variant p.Leu253Pro not only did not activate LPL but rather inhibited

TABLE 3. Functional changes found in apoA-V mutants compared with the wild-type apolipoprotein

	p.(Ser232_Leu235)del	p.Asp332ValfsX4	p.Leu253Pro
Mutation found in controls	No	No	No
Liposome binding	Increased	Increased	Decreased
Heparin binding	Decreased	Decreased	Normal
Interaction with LRP1 cluster II	Yes	Yes	Yes
Interaction with sortilin	Largely impaired	Impaired	No binding
Interaction with SorLA/LR11	No binding	Impaired	No binding
LPL activity	Normal	Normal	Inhibited

the enzyme activity almost completely, a result not observed so far with other recombinantly generated apoA-V mutants (42, 43). This observation clearly points to a direct or indirect effect of this partially disordered mutant on the major lipolytic enzyme. Possible explanations for the observed inhibitory behavior are an impaired lipid binding capacity, which may interfere with enzyme interactions needed for lipolysis, or formation of aggregated structures together with LPL. Other, more speculative hypotheses include promoting conversion of the active homodimeric lipase into inactive monomers, in a similar manner as angiopoietin-like proteins 3 and 4 (53–55), or even a direct blockade of the LPL active site region.

With the exception of R233, the four residues deleted in the novel apoA-V mutant p.(Ser232_Leu235)del are strictly conserved from amphibians to humans, and the S232–L235 tetrapeptide is within or close to a region implicated in the binding of lipids, heparin, and receptors (e.g., GPIHBP1) and also important for LPL activation (19, 21, 56). The recombinant mutant protein showed increased affinity for liposomes but decreased binding to heparin and sortilin, and it did not bind to immobilized SorLA/LR11. By contrast, it interacted with LRP1 cluster II and retained the capacity to activate LPL. The impaired interaction with heparin is not surprising, as this mutation eliminates a pair of consecutive positively charged residues (R233 and K234). In addition to this loss of net positive charge, the four-residue deletion would alter the distance between N- and C-terminal basic residues within this putative HSPG-binding epitope (e.g., R211/R223, on the one hand, and R245/R254 on the other). The combined effect of a lower net charge and the disrupted location of the remaining basic residues would compromise specific protein-proteoglycan interactions. These findings are in line with the previously reported decrease in heparin affinity by mutant p.(Arg233Glu, Lys234Gln) (23). Even more dramatic consequences might be expected for the binding to the N-terminal, highly acidic peptide of GPIHBP1, as indicated by an apoA-V mutant in which residues R233, K234, K238, and K240 were simultaneously replaced by glutamic acid or glutamine residues (56–58).

Inspection of the 3D model suggests deletion of the loop between helices E and F as a further plausible explanation for the deleterious effect of this mutation (Fig. 7B, D). This situation would likely result in an aberrantly long α-helix that spans residues from around V213 to S258, in turn drastically changing the position of the C-terminal region of mutant apoA-V relative to the N-terminal four-helix bundle. Further, hydrophobic residues that are protected from bulk solvent in wild-type apoA-V (mostly leucines, such as L213, L240, L253, and L257) would then form an exposed hydrophobic patch, thereby explaining the higher affinity for liposomes measured in the current work.

Finally, the novel apoA-V mutant p.Asp332ValfsX4 lacks the last 32 C-terminal residues of the protein, which are particularly well conserved in mammals (supplementary Fig. I). Compared with wild-type apoA-V, this variant bound more tightly to liposomes, but it showed impaired interactions with heparin, sortilin, and SorLA/LR11. On the other hand, this mutant showed no detectable changes in the capacity to bind LRP1 cluster II or to activate LPL. The C-terminal region of apoA-V (residues 296–343) has been previously shown to modulate its lipid-binding activity (19, 59). The apparent contradiction with our current results suggests that residues 296–334 play a particularly significant role in this regard.

Both free and DMPC-complexed apoA-V bind LRP1, SorLA/LR11, and sortilin (22), and impaired binding to LDLR family members might lead to hypertriglyceridemia (42). Somewhat unexpectedly in the light of these findings, the three apoA-V mutants were shown to bind to LRP1 cluster II. Even though apoA-V-LRP1 interactions were studied qualitatively, it is unlikely that major changes in receptor affinity could have gone undetected with our ligand blot assay. Along these lines, in similar experiments, the human apoA-V mutants p.(Gln139-Leu147)del, p.Gly185-Cys, p.Glu255Gly, and p.His321Leu bound normally to the chicken LDLR family member LR8, whereas neither the N-terminally truncated apoA-V mutants, p.Gln139× and p.Gln148×, nor a variant prone to multimerization, p.Gly271Cys, were able to bind the avian receptor (42). On the other hand, the pair of basic residues R233/K234 contributes to LRP1 binding, as the double mutant R233E/K234Q showed a 3-fold lower affinity than wild-type apoA-V for the full-length human receptor (23). Altogether, these results suggest that the major LRP1 binding region in apoA-V is located within helices C and D along with the following helix pair, but with little or no contribution from the N- or C-terminal portions of the protein or, in particular, from the last C-terminal residues D332–P366. This binding mode would thus be somewhat similar to the interaction of the related apoE with LDLR (60, 61).

In striking contrast to the retained LRP1-binding ability, the interactions of all three apoA-V variants with sortilin and SorLA/LR11were impaired to different degrees. The crystal structure of the sortilin ectodomain bound to neurotensin reveals a β-propeller module that accommodates the C-terminal residues of the neuropeptide within a deep

internal cavity, which contains additional ligand binding sites (62). On the other hand, C-terminal moieties from other fully unrelated sortilin ligands, such as LPL (25), RAP (63), prosaposin (64), and progranulin (65), are critical for receptor binding. In the light of these findings, it is not surprising that the C-terminally truncated apoA-V variant p.Asp332ValfsX4 binds poorly to SorLA and also showed reduced affinity for sortilin. The observation that mutant p.Leu253Pro did not interact with these receptors is more unexpected and might be explained by an overall collapse of the C-terminal apoA-V region elicited by this point mutation, as discussed above. Our findings reinforce the notion that sortilin and SorLA/LR11 employ different (sub)domains and mechanisms of action for binding the same ligand, as previously shown for LPL (25, 66). In this regard, it must be recalled that, in addition to the common Vps10p domain, SorLA/LR11 contains LA repeats similar to those found in other members of the LDLR family. These ligand binding domains share many ligands with each other, and our current data support the presence of a partly overlapping binding domain in apoA-V, as previously suggested (22). Finally, it is worth noting that both sortilin and SorLA have been shown to facilitate endocytosis of apoA-V-DMPC disks. As SorLA, in contrast to apoA-V, is not primarily expressed in the liver, it is likely that the receptor participates in endocytic functions involving apoA-V rather than in its intracellular processing. Sortilin, on the other hand, is abundantly expressed in the liver; further studies are needed to ascertain whether apoA-V plays a role in VLDL secretion, as recently suggested (67).

In summary, our study strongly suggests a causal relationship between three novel *APOA5* mutations and the hypertriglyceridemia found in the patients through impairment of different apoA-V functions, some of which are of unclear (patho)physiologic significance at this point. Our mutant analysis also provides new clues to the structure-function of apoA-V, a crucial protein in lipoprotein metabolism and cardiovascular risk. In particular, we present for the first time evidence in support of a critical role of the C-terminal region of the apolipoprotein in the interaction with sortilin and, more particularly, with SorLA/LR11.

The authors thank Dr. Morten Nielsen, MIND Center, Aarhus University, Denmark, for kindly providing us with sortilin and SorLA, Dr. Gunilla Olivecrona, Department of Medical Biosciences, Umeå University, Sweden, for providing LPL, and Christine O'Hara for editorial assistance.

REFERENCES

1. Hokanson, J. E., and M. A. Austin. 1996. Plasma triglyceride level is a risk factor for cardiovascular disease independent of high-density lipoprotein cholesterol level: a meta-analysis of population-based prospective studies. *J. Cardiovasc. Risk.* **3:** 213–219.
2. Durrington, P. 2003. Dyslipidaemia. *Lancet.* **362:** 717–731.
3. Wang, J., M. R. Ban, B. A. Kennedy, S. Anand, S. Yusuf, M. W. Huff, R. L. Pollex, and R. A. Hegele. 2008. *APOA5* genetic variants are markers for classic hyperlipoproteinemia phenotypes and hypertriglyceridemia. *Nat. Clin. Pract. Cardiovasc. Med.* **5:** 730–737.
4. Auwerx, J. H., S. P. Babirak, W. Y. Fujimoto, P. H. Iverius, and J. D. Brunzell. 1989. Defective enzyme protein in lipoprotein lipase deficiency. *Eur. J. Clin. Invest.* **19:** 433–437.
5. Breckenridge, W. C., J. A. Little, G. Steiner, A. Chow, and M. Poapst. 1978. Hypertriglyceridemia associated with deficiency of apolipoprotein C-II. *N. Engl. J. Med.* **298:** 1265–1273.
6. Monsalve, M. V., H. Henderson, G. Roederer, P. Julien, S. Deeb, J. J. Kastelein, L. Peritz, R. Devlin, T. Bruin, and M. R. Murthy. 1990. A missense mutation at codon 188 of the human lipoprotein lipase gene is a frequent cause of lipoprotein lipase deficiency in persons of different ancestries. *J. Clin. Invest.* **86:** 728–734.
7. Priore Oliva, C., L. Pisciotta, G. L. Volti, M. P. Sambataro, A. Cantafora, A. Bellocchio, A. Catapano, P. Tarugi, S. Bertolini, and S. Calandra. 2005. Inherited apolipoprotein A-V deficiency in severe hypertriglyceridemia. *Arterioscler. Thromb. Vasc. Biol.* **25:** 411–417.
8. Marçais, C., B. Verges, S. Charrière, V. Pruneta, M. Merlin, S. Billon, L. Perrot, J. Drai, A. Sassolas, L. A. Pennacchio, et al. 2005. ApoA5 Q139X truncation predisposes to late-onset hyperchylomicronemia due to lipoprotein lipase impairment. *J. Clin. Invest.* **115:** 2862–2869.
9. Beigneux, A. P., R. Franssen, A. Bensadoun, P. Gin, K. Melford, J. Peter, R. L. Walzem, M. M. Weinstein, B. S. J. Davies, J. A. Kuivenhoven, et al. 2009. Chylomicronemia with a mutant GPIHBP1 (Q115P) that cannot bind lipoprotein lipase. *Arterioscler. Thromb. Vasc. Biol.* **29:** 956–962.
10. Johansen, C. T., J. Wang, M. B. Lanktree, H. Cao, A. D. McIntyre, M. R. Ban, R. A. Martins, B. A. Kennedy, R. G. Hassell, M. E. Visser, et al. 2010. Excess of rare variants in genes identified by genome-wide association study of hypertriglyceridemia. *Nat. Genet.* **42:** 684–687.
11. Triglyceride Coronary Disease Genetics Consortium and Emerging Risk Factors Collaboration, N. Sarwar, M. S. Sandhu, S. L. Ricketts, A. S. Butterworth, E. di Angelantonio, S. M. Boekholdt, W. Ouwehand, H Watkins, N. J. Samani, et al. 2010. Triglyceride-mediated pathways and coronary disease: collaborative analysis of 101 studies. *Lancet.* **375:** 1634–1639.
12. De Caterina, R., P. J. Talmud, P. A. Merlini, L. Foco, R. Pastorino, D. Altshuler, F. Mauri, F. Peyvandi, D. Lina, S. Kathiresan, et al. 2011. Strong association of the *APOA5*-1131T>C gene variant and early-onset acute myocardial infarction. *Atherosclerosis.* **214:** 397–403.
13. Surendran, R. P., M. E. Visser, S. Heemelaar, J. Wang, J. Peter, J. C. Defesche, J. A. Kuivenhoven, M. Hosseini, M. Péterfy, J. J. P. Kastelein, et al. 2012. Mutations in *LPL, APOC2, APOA5, GPIHBP1* and *LMF1* in patients with severe hypertriglyceridaemia. *J. Intern. Med.* **272:** 185–196.
14. Johansen, C. T., and R. A. Hegele. 2012. The complex genetic basis of plasma triglycerides. *Curr. Atheroscler. Rep.* **14:** 227–234.
15. Pennacchio, L. A., M. Olivier, J. A. Hubacek, J. C. Cohen, D. R. Cox, J-C. Fruchart, R. M. Krauss, and E. M. Rubin. 2001. An apolipoprotein influencing triglycerides in humans and mice revealed by comparative sequencing. *Science.* **294:** 169–173.
16. van der Vliet, H. N., M. G. Sammels, A. C. J. Leegwater, J. H. M. Levels, P. H. Reitsma, W. Boers, and R. A. F. M. Chamuleau. 2001. Apolipoprotein A-V. *J. Biol. Chem.* **276:** 44512–44520.
17. O'Brien, P. J., W. E. Alborn, J. H. Sloan, M. Ulmer, A. Boodhoo, M. D. Knierman, A. E. Schultze, and R. J. Konrad. 2005. The novel apolipoprotein A5 is present in human serum, is associated with VLDL, HDL, and chylomicrons, and circulates at very low concentrations compared with other apolipoproteins. *Clin. Chem.* **51:** 351–359.
18. Alborn, W. E., M. G. Johnson, M. J. Prince, and R. J. Konrad. 2006. Definitive N-terminal protein sequence and further characterization of the novel apolipoprotein A5 in human serum. *Clin. Chem.* **52:** 514–517.
19. Nilsson, S. K., J. Heeren, G. Olivecrona, and M. Merkel. 2011. Apolipoprotein A-V; a potent triglyceride reducer. *Atherosclerosis.* **219:** 15–21.
20. Dichlberger, A., L. A. Cogburn, J. Nimpf, and W. J. Schneider. 2007. Avian apolipoprotein A-V binds to LDL receptor gene family members. *J. Lipid Res.* **48:** 1451–1456.
21. Lookene, A., J. A. Beckstead, S. Nilsson, G. Olivecrona, and R. O. Ryan. 2005. Apolipoprotein A-V-heparin interactions: implications for plasma lipoprotein metabolism. *J. Biol. Chem.* **280:** 25383–25387.
22. Nilsson, S. K., S. Christensen, M. K. Raarup, R. O. Ryan, M. S. Nielsen, and G. Olivecrona. 2008. Endocytosis of apolipoprotein A-V by members of the low density lipoprotein receptor and the Vps10p domain receptor families. *J. Biol. Chem.* **283:** 25920–25927.
23. Nilsson, S. K., A. Lookene, J. A. Beckstead, J. Gliemann, R. O. Ryan, and G. Olivecrona. 2007. Apolipoprotein A-V interaction with members of the low density lipoprotein receptor gene family. *Biochemistry.* **46:** 3896–3904.
24. Stanford, K. I., J. R. Bishop, E. M. Foley, J. C. Gonzales, I. R. Niesman, J. L. Witztum, and J. D. Esko. 2009. Syndecan-1 is the primary heparan

sulfate proteoglycan mediating hepatic clearance of triglyceride-rich lipoproteins in mice. *J. Clin. Invest.* **119:** 3236–3245.
25. Nielsen, M. S., C. Jacobsen, G. Olivecrona, J. Gliemann, and C. M. Petersen. 1999. Sortilin/neurotensin receptor-3 binds and mediates degradation of lipoprotein lipase. *J. Biol. Chem.* **274:** 8832–8836.
26. Jacobsen, L., P. Madsen, C. Jacobsen, M. S. Nielsen, J. Gliemann, and C. M. Petersen. 2001. Activation and functional characterization of the mosaic receptor SorLA/LR11. *J. Biol. Chem.* **276:** 22788–22796.
27. Willnow, T. E., M. Kjølby, and A. Nykjaer. 2011. Sortilins: new players in lipoprotein metabolism. *Curr. Opin. Lipidol.* **22:** 79–85.
28. Strong, A., and D. Rader. 2012. Sortilin as a regulator of lipoprotein metabolism. *Curr. Atheroscler. Rep.* **14:** 211–218.
29. Staden, R., K. F. Beal, and J. K. Bonfield. 2000. The Staden package, 1998. *Methods Mol. Biol.* **132:** 115–130.
30. Civeira, F., M. Pocoví, A. Cenarro, E. Casao, E. Vilella, J. Joven, J. González, A. L. Garcia-Otín, and J. M. Ordovás. 1996. Apo E variants in patients with type III hyperlipoproteinemia. *Atherosclerosis.* **127:** 273–282.
31. Panáková, D., H. Sprong, E. Marois, C. Thiele, and S. Eaton. 2005. Lipoprotein particles are required for Hedgehog and Wingless signalling. *Nature.* **435:** 58–65.
32. Hodnik, V., and G. Anderluh. 2010. Capture of intact liposomes on Biacore sensor chips for protein-membrane interaction studies. *Methods Mol. Biol.* **627:** 201–211.
33. Järving, R., A. Lõokene, R. Kurg, L. Siimon, I. Järving, and N. Samel. 2012. Activation of 11R-lipoxygenase is fully Ca^{2+}-dependent and controlled by the phospholipid composition of the target membrane. *Biochemistry.* **51:** 3310–3320.
34. Karlsson, R., P. S. Katsamba, H. Nordin, E. Pol, and D. G. Myszka. 2006. Analyzing a kinetic titration series using affinity biosensors. *Anal. Biochem.* **349:** 136–147.
35. Merkel, M., B. Loeffler, M. Kluger, N. Fabig, G. Geppert, L. A. Pennacchio, A. Laatsch, and J. Heeren. 2005. Apolipoprotein AV accelerates plasma hydrolysis of triglyceride-rich lipoproteins by interaction with proteoglycan-bound lipoprotein lipase. *J. Biol. Chem.* **280:** 21553–21560.
36. Bengtsson-Olivecrona, G., and T. Olivecrona. 1991. Phospholipase activity of milk lipoprotein lipase. *Methods Enzymol.* **197:** 345–356.
37. Evans, D., J. Aberle, and F. U. Beil. 2011. Resequencing the apolipoprotein A5 (*APOA5*) gene in patients with various forms of hypertriglyceridemia. *Atherosclerosis.* **219:** 715–720.
38. Wong, K., J. A. Beckstead, D. Lee, P. M. M. Weers, E. Guigard, C. M. Kay, and R. O. Ryan. 2008. The N-terminus of apolipoprotein A-V adopts a helix bundle molecular architecture. *Biochemistry.* **47:** 8768–8774.
39. Ajees, A. A., G. M. Anantharamaiah, V. K. Mishra, M. M. Hussain, and H. M. K. Murthy. 2006. Crystal structure of human apolipoprotein A-I: insights into its protective effect against cardiovascular diseases. *Proc. Natl. Acad. Sci. USA.* **103:** 2126–2131.
40. Chen, J., Q. Li, and J. Wang. 2011. Topology of human apolipoprotein E3 uniquely regulates its diverse biological functions. *Proc. Natl. Acad. Sci. USA.* **108:** 14813–14818.
41. Mauldin, K., B. L. Lee, M. Oleszczuk, B. D. Sykes, and R. O. Ryan. 2010. The carboxyl-terminal segment of apolipoprotein A-V undergoes a lipid-induced conformational change. *Biochemistry.* **49:** 4821–4826.
42. Dorfmeister, B., W. W. Zeng, A. Dichlberger, S. K. Nilsson, F. G. Schaap, J. A. Hubacek, M. Merkel, J. A. Cooper, A. Lookene, W. Putt, et al. 2008. Effects of six *APOA5* variants, identified in patients with severe hypertriglyceridemia, on in vitro lipoprotein lipase activity and receptor binding. *Arterioscler. Thromb. Vasc. Biol.* **28:** 1866–1871.
43. Huang, Y-J., Y-L. Lin, C-I. Chiang, C-T. Yen, S-W. Lin, and J-T. Kao. 2012. Functional importance of apolipoprotein A5 185G in the activation of lipoprotein lipase. *Clin. Chim. Acta.* **413:** 246–250.
44. Tai, E. S., and J. M. Ordovas. 2008. Clinical significance of apolipoprotein A5. *Curr. Opin. Lipidol.* **19:** 349–354.
45. Calandra, S., C. Priore Oliva, P. Tarugi, and S. Bertolini. 2006. APOA5 and triglyceride metabolism, lesson from human APOA5 deficiency. *Curr. Opin. Lipidol.* **17:** 122–127.
46. Pisciotta, L., R. Fresa, A. Bellocchio, V. Guido, C. P. Oliva, S. Calandra, and S. Bertolini. 2011. Two novel rare variants of *APOA5* gene found in subjects with severe hypertriglyceridemia. *Clin. Chim. Acta.* **412:** 2194–2198.
47. Hubacek, J. A., W-W. Wang, Z. Škodová, V. Adámková, M. Vráblík, A. Hořinek, T. Štulc, R. Češka, and P. J. Talmud. 2008. *APOA5* Ala315>Val, identified in patients with severe hypertriglyceridemia, is a common mutation with no major effects on plasma lipid levels. *Clin. Chem. Lab. Med.* **46:** 773–777.
48. Oda, M. N., T. M. Forte, R. O. Ryan, and J. C. Voss. 2003. The C-terminal domain of apolipoprotein A-I contains a lipid-sensitive conformational trigger. *Nat. Struct. Biol.* **10:** 455–460.
49. Silva, R. A. G. D., R. Huang, J. Morris, J. Fang, E. O. Gracheva, G. Ren, A. Kontush, W. G. Jerome, K-A. Rye, and W. S. Davidson. 2008. Structure of apolipoprotein A-I in spherical high density lipoproteins of different sizes. *Proc. Natl. Acad. Sci. USA.* **105:** 12176–12181.
50. Lund-Katz, S., D. Nguyen, P. Dhanasekaran, M. Kono, M. Nickel, H. Saito, and M. C. Phillips. 2010. Surface plasmon resonance analysis of the mechanism of binding of apoA-I to high density lipoprotein particles. *J. Lipid Res.* **51:** 606–617.
51. Huang, R., R. A. G. D. Silva, W. G. Jerome, A. Kontush, M. J. Chapman, L. K. Curtiss, T. J. Hodges, and W. S. Davidson. 2011. Apolipoprotein A-I structural organization in high-density lipoproteins isolated from human plasma. *Nat. Struct. Mol. Biol.* **18:** 416–422.
52. Charrière, S., C. Cugnet, M. Guitard, S. Bernard, L. Groisne, M. Charcosset, V. Pruneta-Deloche, M. Merlin, S. Billon, M. Delay, et al. 2009. Modulation of phenotypic expression of *APOA5* Q97X and L242P mutations. *Atherosclerosis.* **207:** 150–156.
53. Sukonina, V., A. Lookene, T. Olivecrona, and G. Olivecrona. 2006. Angiopoietin-like protein 4 converts lipoprotein lipase to inactive monomers and modulates lipase activity in adipose tissue. *Proc. Natl. Acad. Sci. USA.* **103:** 17450–17455.
54. Shan, L., X-C. Yu, Z. Liu, Y. Hu, L. T. Sturgis, M. L. Miranda, and Q. Liu. 2009. The angiopoietin-like proteins ANGPTL3 and ANGPTL4 inhibit lipoprotein lipase activity through distinct mechanisms. *J. Biol. Chem.* **284:** 1419–1424.
55. Lee, E. C., U. Desai, G. Gololobov, S. Hong, X. Feng, X-C. Yu, J. Gay, N. Wilganowski, C. Gao, L-L. Du, et al. 2009. Identification of a new functional domain in angiopoietin-like 3 (ANGPTL3) and angiopoietin-like 4 (ANGPTL4) involved in binding and inhibition of lipoprotein lipase (LPL). *J. Biol. Chem.* **284:** 13735–13745.
56. Gin, P., L. Yin, B. S. J. Davies, M. M. Weinstein, R. O. Ryan, A. Bensadoun, L. G. Fong, S. G. Young, and A. P. Beigneux. 2008. The acidic domain of GPIHBP1 is important for the binding of lipoprotein lipase and chylomicrons. *J. Biol. Chem.* **283:** 29554–29562.
57. Beigneux, A. P., B. S. J. Davies, P. Gin, M. M. Weinstein, E. Farber, X. Qiao, F. Peale, S. Bunting, R. L. Walzem, J. S. Wong, et al. 2007. Glycosylphosphatidylinositol-anchored high-density lipoprotein-binding protein 1 plays a critical role in the lipolytic processing of chylomicrons. *Cell Metab.* **5:** 279–291.
58. Shu, X., L. Nelbach, M. M. Weinstein, B. L. Burgess, J. A. Beckstead, S. G. Young, R. O. Ryan, and T. M. Forte. 2010. Intravenous injection of apolipoprotein A-V reconstituted high-density lipoprotein decreases hypertriglyceridemia in *apoav*−/− mice and requires glycosylphosphatidylinositol-anchored high-density lipoprotein-binding protein 1. *Arterioscler. Thromb. Vasc. Biol.* **30:** 2504–2509.
59. Beckstead, J. A., K. Wong, V. Gupta, C-P. L. Wan, V. R. Cook, R. B. Weinberg, P. M. M. Weers, and R. O. Ryan. 2007. The C terminus of apolipoprotein A-V modulates lipid-binding activity. *J. Biol. Chem.* **282:** 15484–15489.
60. Wilson, C., M. R. Wardell, K. H. Weisgraber, R. W. Mahley, and D. A. Agard. 1991. Three-dimensional structure of the LDL receptor-binding domain of human apolipoprotein E. *Science.* **252:** 1817–1822.
61. Weisgraber, K. H. 1994. Apolipoprotein E: structure-function relationships. *Adv. Protein Chem.* **45:** 249–302.
62. Quistgaard, E. M., P. Madsen, M. K. Groftehauge, P. Nissen, C. M. Petersen, and S. S. Thirup. 2009. Ligands bind to Sortilin in the tunnel of a ten-bladed [beta]-propeller domain. *Nat. Struct. Mol. Biol.* **16:** 96–98.
63. Tauris, J., L. Ellgaard, C. Jacobsen, M. S. Nielsen, P. Madsen, H. C. Thøgersen, J. R. Gliemann, C. M. Petersen, and S. R. K. Moestrup. 1998. The carboxy-terminal domain of the receptor-associated protein binds to the Vps10p domain of sortilin. *FEBS Lett.* **429:** 27–30.
64. Yuan, L., and C. R. Morales. 2010. A stretch of 17 amino acids in the prosaposin C terminus is critical for its binding to sortilin and targeting to lysosomes. *J. Histochem. Cytochem.* **58:** 287–300.
65. Zheng, Y., O. A. Brady, P. S. Meng, Y. Mao, and F. Hu. 2011. C-terminus of progranulin interacts with the beta-propeller region of sortilin to regulate progranulin trafficking. *PLoS ONE.* **6:** e21023.
66. Klinger, S. C., S. Glerup, M. K. Raarup, M. C. Mari, M. Nyegaard, G. Koster, T. Prabakaran, S. K. Nilsson, M. M. Kjaergaard, O. Bakke, et al. 2011. SorLA regulates the activity of lipoprotein lipase by intracellular trafficking. *J. Cell Sci.* **124:** 1095–1105.
67. Strong, A., Q. Ding, A. C. Edmondson, J. S. Millar, K. V. Sachs, X. Li, A. Kumaravel, M. Y. Wang, D. Ai, L. Guo, et al. 2012. Hepatic sortilin regulates both apolipoprotein B secretion and LDL catabolism. *J. Clin. Invest.* **122:** 2807–2816.